

This is the Author's Pre-print version of the following article: *Jose de Jesus Esquivel-Gómez, Juan Gonzalo Barajas-Ramírez. Efficiency of quarantine and self-protection processes in epidemic spreading control on scale-free networks Chaos 28, 013119 (2018)*; which has been published in final form at: <https://doi.org/10.1063/1.5001176>

1 **Efficiency of quarantine and self-protection processes in epidemic spreading control**  
 2 **on scale-free networks**

3 J. Esquivel-Gómez<sup>1, a)</sup> and J. G. Barajas-Ramírez<sup>1, b)</sup>

4 *Instituto Potosino de Investigación Científica y Tecnológica (IPICYT)*

5 *División de Matemáticas Aplicadas.*

6 *Camino a la Presa San José 2055,*

7 *Col. Lomas 4a Secc. C.P.78216.*

8 *San Luis Potosí, SLP, México.*

9 (Dated: 11 November 2017)

10 One of the most effective mechanisms to contain the spread of an infectious disease  
 11 through a population is the implementation of quarantine policies. However, its effi-  
 12 ciency is affected by different aspects, for example, the structure of the underlining  
 13 social network where highly connected individuals as the more likely to become in-  
 14 fected, therefore the speed of the transmission of the decease is directly determine by  
 15 degree distribution of the network. Another, aspect that influences the effectiveness  
 16 of the quarantine is the self-protection processes of the individuals in the popula-  
 17 tion, that is, they try to avoid contact with potentially infected individuals. In this  
 18 paper we investigate the efficiency of quarantine and self-protection processes in pre-  
 19 venting the spreading of infectious diseases over complex networks with a power-law  
 20 degree distribution ( $P(k) \sim k^{-\nu}$ ) for different  $\nu$  values. We propose two alternative  
 21 scale-free models that result in power-law degree distributions above and below the  
 22 exponent  $\nu = 3$  associated with the conventional Barabási-Albert model. Our results  
 23 show that the exponent  $\nu$  determines the effectiveness of these policies on controlling  
 24 the spreading process. More precisely, we show that for  $\nu$  exponent below three, the  
 25 quarantine mechanism loses effectiveness. However, the efficiency is improved if the  
 26 quarantine is jointly implemented with a self-protection process driving the number  
 27 of infected individual significantly lower.

28 **Keywords:** Complex networks, spread of diseases, quarantine, scale-free networks

---

<sup>a)</sup>Electronic mail: jose.esquivel@ipicyt.edu.mx

<sup>b)</sup>Electronic mail: jgbarajas@ipicyt.edu.mx

29 Infectious diseases are by far one of the leading causes of death worldwide.  
30 In this sense, one of the most effective mechanisms to contain the spread of an  
31 infectious disease in a population is the implementation of quarantine policies.  
32 However, other aspects must be considered, for example, degree distribution of  
33 the underlining social network points towards the most connected individuals as  
34 the more likely to become infected and determine the speed of the transmission  
35 of the disease. Additionally, self-protection processes influence the individuals  
36 in the population resulting on alterations in their behavior, in particular they try  
37 to avoid contact with potentially infected individuals. In this paper, we inves-  
38 tigate the efficiency of quarantine and self-protection processes as controllers  
39 of the spreading of infections in power-law networks with degree distribution  
40 below and above the exponent of the classic Barabási-Albert model. Our results  
41 show that the efficiency of these control processes does depend directly on the  
42 exponent of the degree distribution with the quarantine being less effective in  
43 controlling the infection on networks with low degree distributions exponents.  
44 However, the inclusion of the self-protection process compensates this effect and  
45 further increases the effectiveness of the control process. These results imply  
46 that a good strategy to avoid the emergence of epidemics is the awareness of the  
47 population of its presence through social communication programs to activate a  
48 self-protection process along with the quarantine protocol.

## 49 I. INTRODUCTION

50 In recent years, evolutionary dynamics in complex networks have attracted the attention  
51 of researchers of different areas. In particular, with regards to their effect on the resulting  
52 dynamical features of their collective behaviors, such as synchronization or consensus<sup>1-3</sup>. In  
53 this sense, epidemic spreading can be modeled as a process occurring on top of a contact  
54 network with a given structure, be it fixed, time-varying, having stochastic or even multi-  
55 network features<sup>4-7</sup>. As such, major contributions have been made in the mathematical  
56 description of how a computer virus spreads in a network of computers, or how a rumor  
57 becomes entrenched within a social network; which in turn have impacted the way we model  
58 the spread of diseases in our population<sup>8,10</sup>. Moreover, the use of mathematical models better

59 informs the determination of the control measures that need to be taken to stop a disease  
60 from spreading. A considerable number of epidemic models have been proposed, the majority  
61 of them use the concept of population compartments<sup>11</sup>. That is, the population is partition  
62 into different compartments accordingly to health status<sup>4,12</sup>, for example: Susceptible ( $S$ ,  
63 the group of individual that can contract the disease), Exposed ( $E$ , made of individuals  
64 that have been infected but are not infectious, that is, they are in a latent period of the  
65 disease), Infected ( $I$ , individuals that can infect susceptible individuals), and Removed ( $R$ ,  
66 the part of the population that have recovered from the disease and can not become infected  
67 again or individuals that have died). The mathematical models describe the evolution  
68 of the concentrations of these compartments usually under the assumption of a fixed size  
69 population. Additionally, in several epidemic models the use of control mechanisms to  
70 contain the spread of a disease is considered. In this sense, the effect of using a vaccination  
71 or a quarantine scheme on the evolution of the disease can be evaluated in terms of the  
72 number of infected individuals after the infection process has run its course.

73 Classical epidemic models consider that the population is totally homogeneous<sup>11–13</sup>. In  
74 other words, all individuals have the same probability of contracting the disease, recover from  
75 it, or die. As such a constant average rate of infection and recovery can be use for the entire  
76 population. However, in a real scenario individuals who interact with a greater number of  
77 individuals are more likely to contract a disease than individuals that are relatively isolated  
78 from their neighbors. In short, the distribution of connection within a population has a  
79 great influence in the spreading process of a disease. For this reason, it is important to take  
80 into account the degree of interaction of each individual in determining its probability of  
81 contracting a disease. One way to incorporate the complex topology of social networks in  
82 epidemic models is to consider its degree distribution, that is, the number of connections of  
83 each node has. Recent investigation have confirm that the degree distribution of a social  
84 network is well described by a power-law  $P(k) \sim k^{-\nu}$ . Therefore, its characteristics can be  
85 use to establish the probability of infection for each node in the network. This allows to take  
86 into account the existence of a few “hub” individuals that concentrate a greater number and  
87 therefore are the main contributors of the spreading of the disease, while the contribution to  
88 the spread of the majority of the individuals with a relatively low number of connections is  
89 less significant. In this context, a particularly interesting investigation was reported by Liu  
90 and Zhang<sup>17</sup>, where in order to investigate the influence of heterogeneity of the network on

91 the epidemic spreading of a disease, the underlining social network was modeled as a scale-  
 92 free network generated with the Barabási-Albert (*BA*) model<sup>16</sup>. That is, the underlining  
 93 social network was modeled as a non-directed network with degree distribution that follows a  
 94 power-law  $P(k) \sim k^{-\nu}$  with a fixed exponent  $\nu = 3$ . In the work by Li *et al.*<sup>15</sup> the quarantine  
 95 control mechanism was also considered in the epidemic model, the proposed model was called  
 96 *SIQRS*, to indicate the different compartments of the population, with *Q* referring to the  
 97 infected individuals placed in quarantine. The effectiveness of the quarantine strategy in  
 98 stopping the spread of the disease was measured by the authors in terms of the density of  
 99 infected nodes in steady state ( $I^\infty$ ), they showed that  $I^\infty$  decreases as the quarantine rate  
 100 increases. However, the effect that different exponents  $\nu$  have on the density of infected  
 101 nodes in steady state  $I^\infty$  was not investigated. As the exponent of the degree distribution  
 102 gives a clear indication of the formation of hub nodes in the network and these are the  
 103 individuals that promote the spreading of the disease, it stands to reason that the degree  
 104 distribution exponent is also a determining factor in the efficiency of the quarantine policy  
 105 in stopping epidemic spreading. Another assumption in<sup>15</sup>, is that only infected individuals  
 106 can be quarantined. However, in a real scenario individuals tend to protect themselves by  
 107 temporally avoiding contacts with infected individuals that is, individuals can quarantine  
 108 themselves (*self-quarantine* process) or in other situations, the individuals can permanently  
 109 disconnect from their infected neighbors (*deleting-infected-links* process).

110 In order to investigate the quarantine and self-protection processes effectiveness in stop-  
 111 ping the epidemic spreading, in this paper we investigate the steady state solutions of the  
 112 *SIQRS* model over complex networks with different  $\nu$  values. Considering three cases. In  
 113 the first, we define quarantine as the only control action. In the second, we implement  
 114 the quarantine jointly with a *self-quarantine* process. Finally, the quarantine in joint with  
 115 *deleting-infected-links* process is implemented. Our results show that as the  $\nu$  exponent  
 116 decreases, the density of infected individuals in steady state increases for all the cases. In  
 117 other words, the control mechanisms lose effectiveness as the  $\nu$  exponent decreases. This is  
 118 particularly significant when one consider that social networks do not have a fixed power  
 119 law distribution exponent, and it definitely is not exactly equal to three<sup>18</sup>. However the best  
 120 results are obtained when both a quarantine and a *self-protection* processes are implemented.

121 As mentioned above, in recent years, several works about the spread of diseases in complex  
 122 networks have been published. For example, in<sup>19</sup>, Shang *et.al.* study the effect of changes

123 on the network structure in the spread of disease using the well known SIS model. In  
124 particular, they study the effect of the community structure over the spread. They found  
125 that, epidemics spread faster on networks with higher level of overlapping communities and  
126 degree distributions with power law exponents equals to two and three. In<sup>5-7</sup> the SIS model  
127 was also considered, but analyzing the effect of the awareness diffusion in the network, and  
128 they found that the awareness diffusion plays an important role in the epidemic transmission.  
129 In these published works, the numerical experiments are based in complex networks with a  
130 fixed power-law exponent equal to 2.5. In this paper, we consider that the topology is fixed  
131 during the spread and the awareness is adopted by the individuals that can be in contact  
132 with the infected. Another important difference is that we analyze the effect of different  
133 power-law exponents in the spreading dynamics of the disease. To his end, in the following  
134 Section two alternative versions of the BA model are presented which will be the basis for  
135 our investigation on the efficiency of quarantine and self-protection as control processes of  
136 the spreading dynamics

137 The remainder of this paper is organized as follows. An alternative scale-free network  
138 model where the degree distribution exponent can be assign to be larger or smaller that  
139 three are described in Section II. While the *SIQRS* epidemic model along with the analysis  
140 of the effect of the underlining degree distribution is presented in Section III. Our results  
141 and numerical simulations are shown in Section IV. Finally, our results and conclusions are  
142 discussed in Section V.

## 143 **II. PROPOSED NETWORK MODELS WITH A PRESCRIBED DEGREE** 144 **DISTRIBUTION**

145 In order to investigate the efficiency of the quarantine policy to contain the spread of  
146 disease on scale free networks, we propose two network models with power law degree dis-  
147 tributions where the exponents is in the range  $1 < \nu < 6$ . These models are described  
148 bellow:

### 149 **A. Model I. Network with an exponent less than three**

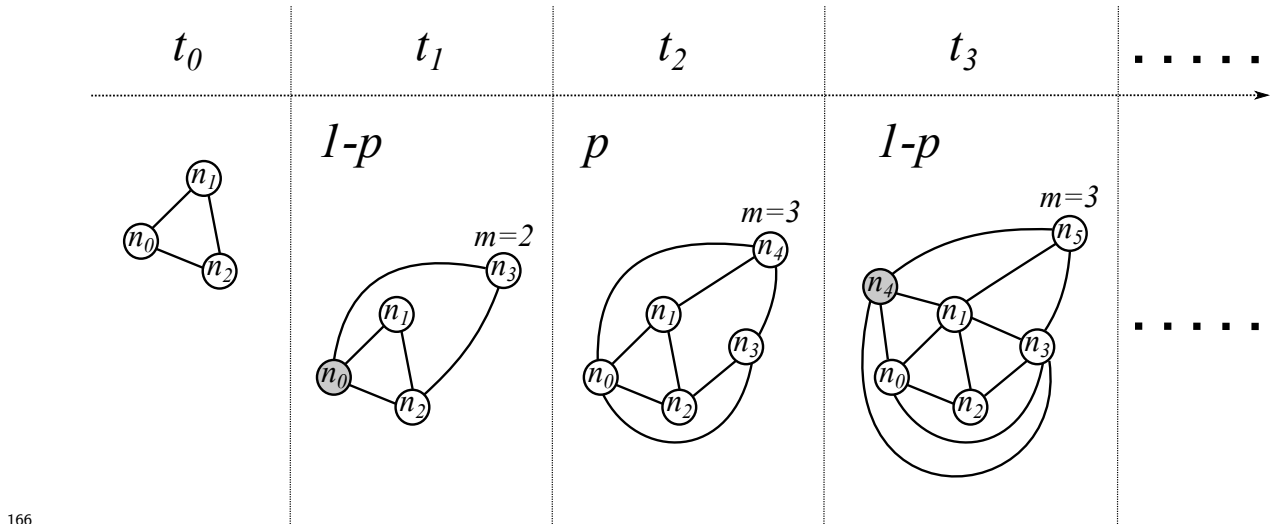
150 In a similar way as the classical *BA* model, our proposed model consists of two steps:

- 151 1. **Growth:** Starting from a set of three fully connected nodes at each subsequent time  
 152 step one node is added, and
- 153 2. **Preferential attachment:** In our model the links between the new node and those  
 154 already existing in the network are added according to the following rules:
- 155 a. With probability  $p$  the new node  $n_{new}$  is connected with  $m = 3$  links, and with  
 156 the complementary probability  $1 - p$  the number of links of the new node  $n_{new}$   
 157 is taken to be the node degree of a randomly selected node in the network;
- 158 b. The number of links determine in the previous step connect  $n_{new}$  node to different  
 159 nodes already existing in the network with a probability given by

$$160 \quad \Pi(n_i) = \frac{k_i}{\sum_j k_j}, \quad (1)$$

161 where  $k_i$  is the degree of the node  $n_i$  and  $\Pi(n_i)$  describes the probability that  
 162 node  $n_i$  gets a new link.

163 It is worth noting that (1) is similar to the attachment probability proposed in the original  
 164 BA model<sup>16</sup>. However, by changing the number of connections our proposed model produces  
 165 networks with degree distribution that follows a power-law with an exponent  $\nu \leq 3$ .



167 FIG. 1. Growth (from  $t_0$  to  $t_3$ ) of a network using the Model I. In the Figure the circles represent  
 168 nodes of the network, the solid lines links and filled circles nodes that have been randomly selected  
 169 to copy their degree for the new node.

170 The growth process of a network using the proposed Model 1 is shown in Figure 1. In  
171 the first time step  $t_0$ , the network consists of three nodes  $n_0$ ,  $n_1$  and  $n_2$ . In the next time  
172 step  $t_1$ , the node  $n_3$  is added to the network lets assumed that it copies the degree from the  
173 node  $n_0$  which is selected randomly. Then, node  $n_3$  is connected randomly to  $m = 2$  of the  
174 existing nodes in the network with probability 1. In the figure it is assumed that the node  
175  $n_3$  connects to nodes  $n_0$  and  $n_2$ . In time step  $t_2$ , the node  $n_4$  is added to the network and  
176 in this case se assume that  $m = 3$ , then is connected randomly to the nodes  $n_0$ ,  $n_1$  and  $n_3$ .  
177 In  $t_3$ , the node  $n_5$  is added to the network and it is assumed that it copies the degree from  
178 the node  $n_4$  and connects to the nodes  $n_1$ ,  $n_3$  and  $n_4$ . This process is continued for all the  
179 following time steps until the number of nodes in the network is sufficiently large and the  
180 structural properties of the network become fixed.

181 In order to get the behavior of the mean degree  $\bar{k}$  as the network growth in the proposed  
182 model, we propose the following differential equation,

$$183 \quad \frac{d\bar{k}(N)}{dN} = p \frac{2m - \bar{k}}{N} + (1 - p)p \frac{2\bar{k} - \bar{k}}{N}. \quad (2)$$

184 with the initial condition  $\bar{k}(3) = 2$ , which describes the initial network of three nodes fully  
185 connected; one gets,

$$186 \quad \bar{k}(N) = 2mp \left[ \frac{1}{2p - 1} - \frac{p + 1}{(2p - 1)p3^{2(1-p)}} N^{1-2p} \right]. \quad (3)$$

187 In Figure 2 we show the degree distribution  $P(k)$  and the average degree  $\langle k \rangle$  obtained from  
188 two different realizations of Model I. For each one, the network was growth to  $N = 10000$   
189 nodes. In the first realization the probability of having  $m = 3$  links for each new node is set  
190 at  $p = 0.3$ , for the second realization the probability was  $p = 0.7$ . As shown in Figures 2a  
191 and 2b, the degree distribution of the generated network follows a power law with exponents  
192  $\nu \sim 1.4$  for  $p = 0.3$  and  $\nu \sim 2.3$  for  $p = 0.7$ . It is also important to mention that for  $p = 0.3$   
193 the average degree grows more rapidly than for  $p = 0.7$  (see Figures 2c and 2d), this indicates  
194 that as the value of  $p$  decreases the network becomes to be more densely connected.

## 195 B. Model II: Network with an exponent larger than three

196 As before the network model consist of two steps. The network growths one node each  
197 time step beginning with three fully connected nodes. However, in this model each new



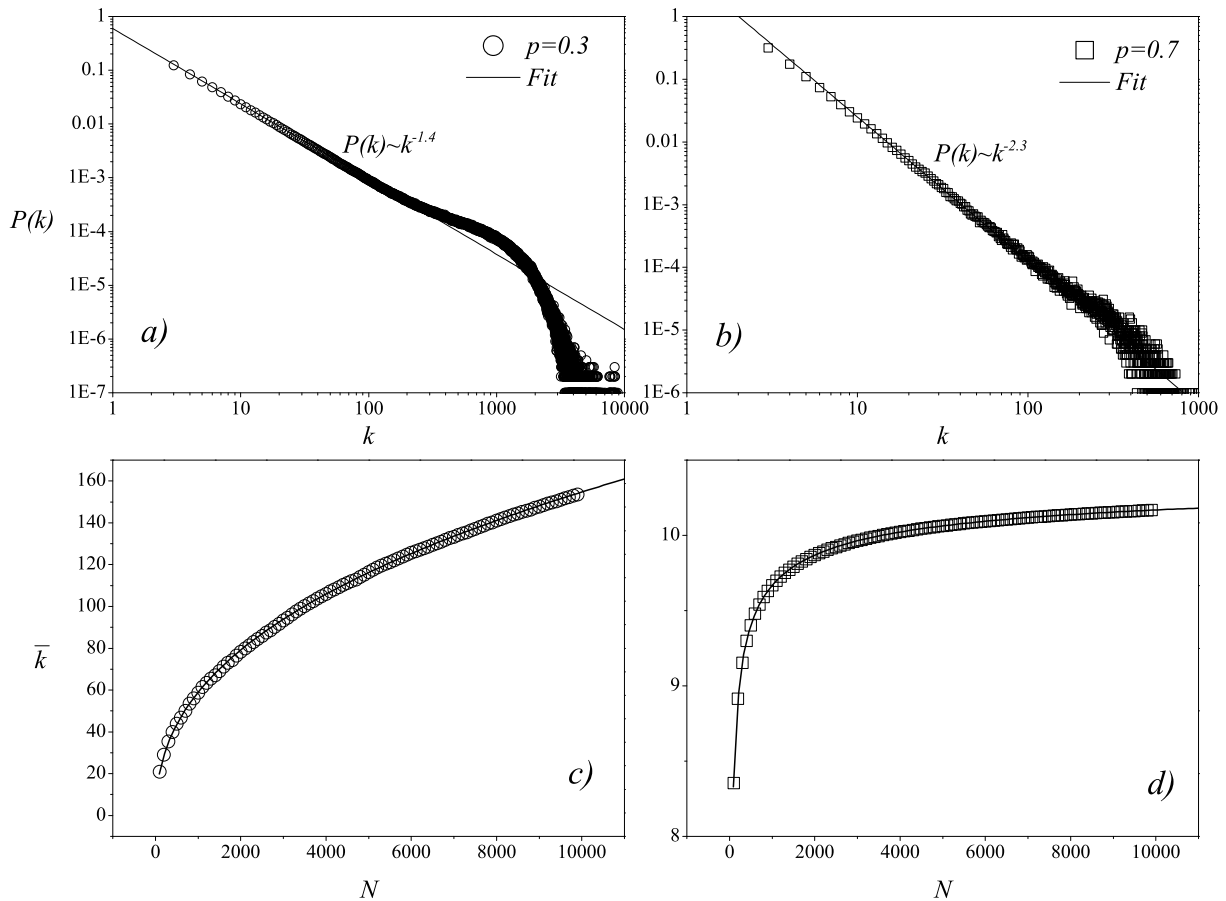


FIG. 2. a) Degree distribution and c) Average degree. Both measured at different sizes of the generated network using Model I with  $p = 0.3$ . b) Degree distribution and d) Average degree. Measured at different sizes of the generated network using Model I with  $p = 0.7$ .

198 node is born with the maximum number of links possible  $m = 3$  and with an attractiveness  
 199 factor  $A \geq 0$ , which is equal for all the nodes in the network. In the second step, the links of  
 200 each new node are connected to different nodes already in the network using the attachment  
 201 probability given by

$$202 \quad \Pi(n_i) = \frac{k_i + A}{\sum_j (k_j + A)}, \quad (4)$$

203 where  $k_i$  is the degree of a node  $n_i$  and  $A$  is the initial attractiveness of the nodes in the  
 204 network. Due to the addition of links is constant at each time step, the last equation can  
 205 be written as:

206

$$\Pi(n_i) = \frac{k_i + A}{(2m + A)N}. \quad (5)$$

207

208

209

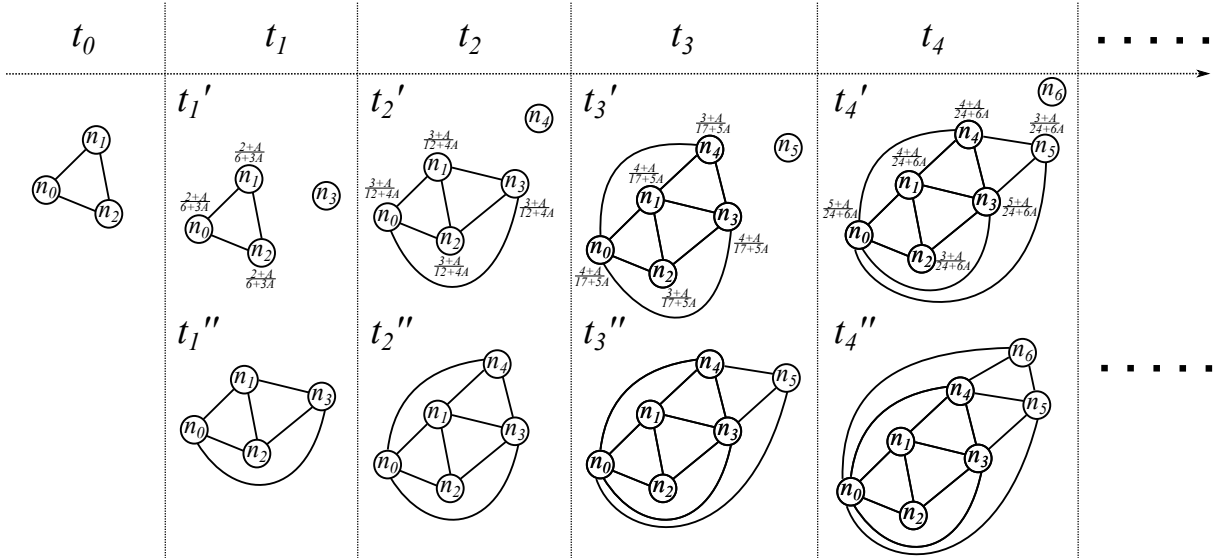
210

211

This version of the scale-free model is inspired by the model proposed by Dorogovtsev and Mendez<sup>20</sup>, using the attractiveness factor  $A$  the resulting scale-free network can be made to have a degree distribution exponent  $\nu \geq 3$ . In order to obtain the analytical solution for  $P(k)$  in this model, it is necessary to know the number  $Q_i$  of nodes with  $i$  links with respect to the total number  $N$  of nodes in the network, that is,

212

$$P(k) = \frac{Q_i(N)}{N} \quad (6)$$



213

214

215

216

FIG. 3. Growth of a network using the Model II from  $t_0$  to  $t_4$ . In the Figure the circles represent to the nodes of the network and the solid lines to the links. It also shows the probability  $\Pi$  for each node.

217

218

To get an expression for  $Q_i(N)$ , the continuum method<sup>21</sup> was employed using the following differential equation:

219

220

221

$$\frac{dQ_i(N)}{dN} = m \frac{\overbrace{(i-1+A)Q_{i-1}(N)}^{g_1}}{(2m+A)N} - m(i-1) \frac{\overbrace{(i+A)Q_i(N)}^{g_2}}{(2m+A)N} + \overbrace{\delta_{i,m}}^{g_3}. \quad (7)$$

222 The variation of the number  $Q_i$  of nodes with  $i$  links with respect to the number  $N$   
 223 of nodes in the network is described by (7). The term  $g_1$  represents how the number of  
 224 nodes with  $i$  links increases and the term  $g_2$  describes how the number of nodes with  $i$  links  
 225 decreases. Finally, the term  $g_3$  models the effect of adding a new node with  $m$  links.

226 In order to obtain  $Q_i(N)$ , Eq. 7 is solved for  $i = m$ ,  $i = m + 1$ , and so on. For  $i = m$ ,  
 227 (7) takes the form,

$$228 \quad \frac{dQ_m(N)}{dN} = -\frac{m(m+A)}{(2m+A)N}Q_m + 1. \quad (8)$$

229 Solving (8), we obtain

$$230 \quad Q_m(N) = \frac{2m+A}{m(m+A)+(2m+A)}N. \quad (9)$$

231 For the following  $i$  value produces:

$$232 \quad Q_{m+1} \approx \frac{m(m+A)(2m+A)}{[m(m+A)+(2m+A)][m(m+1+A)+(2m+A)]}N$$

$$233 \quad Q_{m+2}(N) \approx \frac{m(m+A)m(m+1+A)(2m+A)}{[m(m+A)+(2m+A)][m(m+1+A)+(2m+A)]}$$

$$234 \quad \frac{1}{[m(m+2+A)+(2m+A)]}N,$$

$$235 \quad \frac{1}{[m(m+2+A)+(2m+A)]}N, \quad (10)$$

238 with the last results we can deduce,

$$239 \quad Q_i(N) \approx (2m+A) \frac{\prod_{x=m}^{i-1} [m(x+A)]N}{\prod_{x=m}^i [m(x+A)+2m+A]}$$

$$240 \quad \approx \frac{(2m+A)\Gamma(2+A+\frac{A}{m}+m)N}{m\Gamma(m+A)}(i+A)^{-(3+\frac{A}{m})}.$$

$$241 \quad (11)$$

Then, the degree distribution  $P(k)$  obtained with the proposed model has the form

$$P(k) \sim i^{-(3+\frac{A}{m})}$$

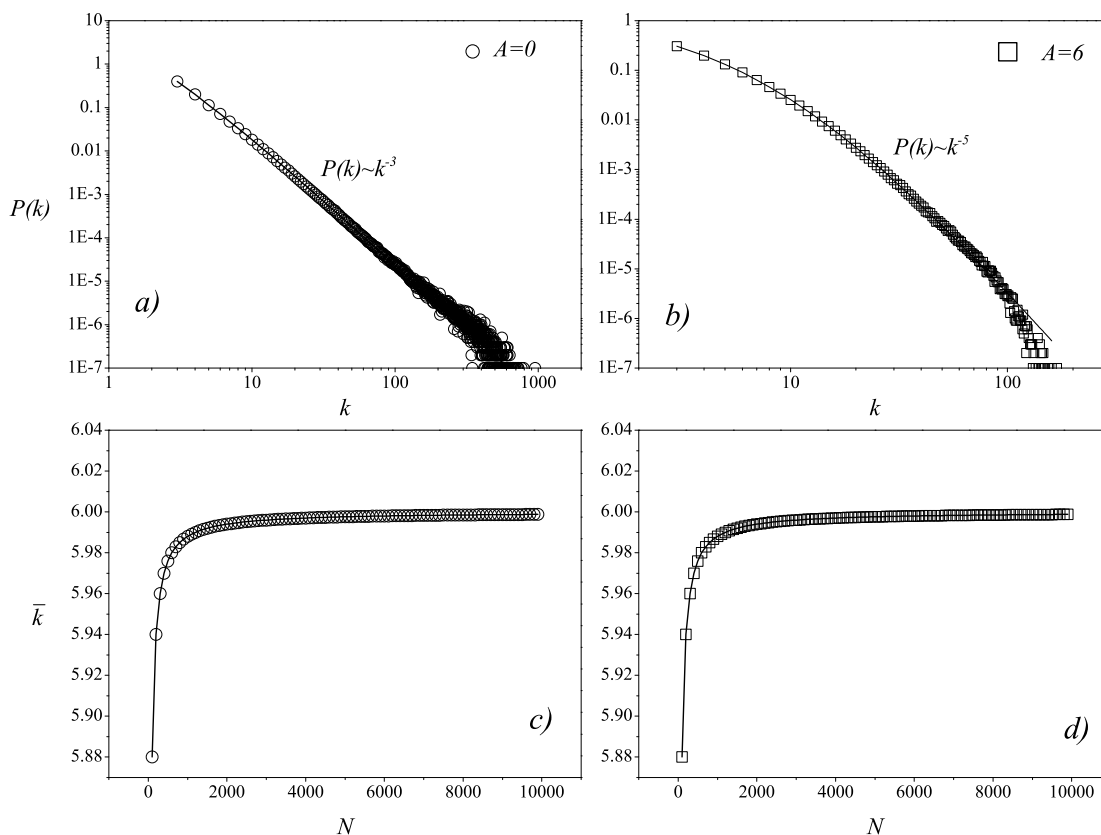
242 decaying as a power law with exponent  $\nu \geq 3$ . Another important characteristic of a growth  
 243 model is to know the mean degree  $\bar{k}$  as the network growth. For the model,  $\bar{k}$  can be obtained  
 244 solving the following differential equation,

$$245 \quad \frac{d\bar{k}(N)}{dN} = \frac{2m - \bar{k}}{N}. \quad (12)$$

246 with the initial condition  $\bar{k}(3) = 2$  that describes the initial network consisting of three  
 247 nodes fully connected. Which yields,

$$248 \quad \bar{k}(N) = 2m + \frac{3(2 - 2m)}{N}. \quad (13)$$

249 Figure 3 shows the growth of a network with the Model II. As can be seen, in the first time



250

251 FIG. 4. a) Degree distribution and c) Average degree measured at different sizes of the generated  
 252 network using Model II with  $A = 0$ . b) Degree distribution and d) Average degree measured at  
 253 different sizes of the generated network using Model II with  $A = 6$ .

254  
 255

256 step  $t_0$ , the network consists of three nodes  $n_0$ ,  $n_1$  and  $n_2$ . In the next time step  $t_1$ , the

257 node  $n_3$  is added to the network and the probabilities from nodes in the network to get a  
 258 new link from  $n_3$  are showed in  $t'_1$ , in this case all nodes have the same probability and it  
 259 is assumed that  $n_3$  connects to all ( $t''$ ). A similar process occur in  $t_2$  and  $t_3$ . However, in  
 260  $t'_4$  it is possible to see that difference in the probabilities of nodes  $n_0$  to  $n_5$  depend of the  $A$   
 261 value. That is, as the value of  $A$  becomes to be greater the probabilities for the nodes tends  
 262 to be more uniform and as the network grows the emergence of hub nodes is less frequent.  
 263 In Figure 4 are showed the degree distribution  $P(k)$  and the average degree  $\bar{k}$  obtained  
 264 from two different realization of the model. Each realization of the network was grown to  
 265  $N = 10000$  nodes for the first realization  $A = 0$ , while for the second the attractiveness value  
 266 was set to  $A = 6$ . As shown in Figures 4a and 4b, the degree distribution of the generated  
 267 network follows a power law with exponent  $\nu \sim 3$  for  $A = 0$  and  $\nu \sim 5$  for  $A = 6$ . Also, it  
 268 is important to mention that the average degree has the same behavior in both cases (see  
 269 Figs. 4c and 4d), that is  $\langle k \rangle \sim 6$  as  $N \gg 1$  in both cases.

### 270 III. QUARANTINE AND *SELF-PROTECTION* PROCESSES

271 In this section we investigate the quarantine and *self-protection* processes efficiency to  
 272 stop the epidemic spreading in networks with the structure given by Models I and II. We  
 273 study three cases:

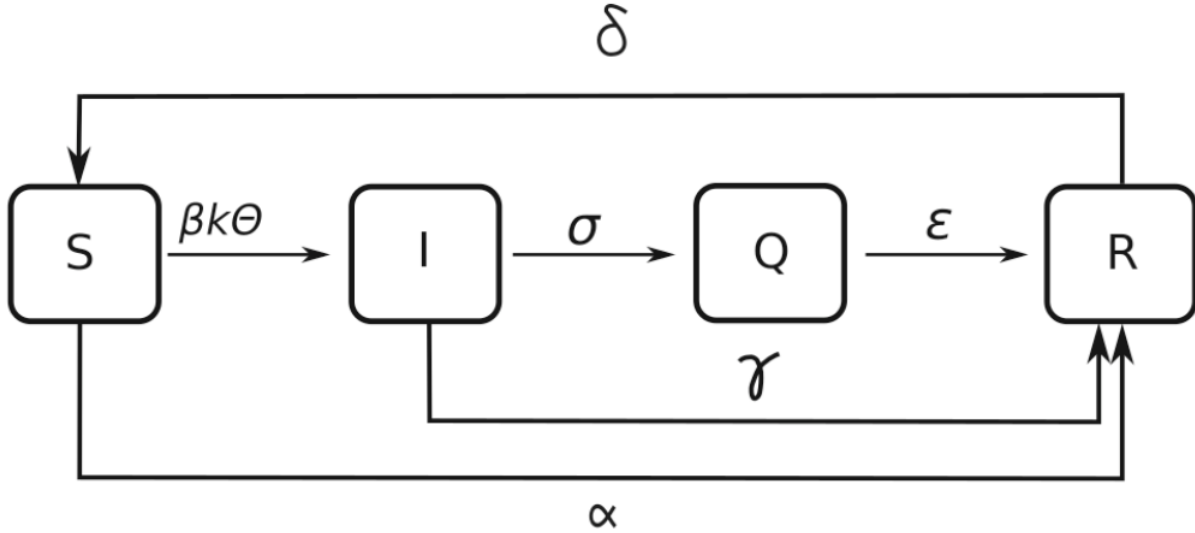
#### 274 A. Quarantine as the only control action

275 In order to contain the spread of infectious diseases, one of the most effective control  
 276 actions is the quarantine policy, that consists in isolate several infected individuals to im-  
 277 paired the contagion process and reduce the emergence of new infected individuals. In this  
 278 section is considered an epidemic model that implements the quarantine as a control action.  
 279 In particular, we focus in a *SIQRS* model and analyze its efficiency in scale-free networks  
 280 with different degree distributions. In the model, it is assumed that the network consist  
 281 in  $N$  nodes and each node of the network can only exist in one of the four discrete states,  
 282 namely, susceptible, infected, quarantined or removed, and the infection spreads over the  
 283 links of the network. Another assumption is that the population is fixed, that is, births and

284 deaths of nodes are not considered, and thus

$$285 \quad S(t) + I(t) + Q(t) + R(t) = 1, \quad (14)$$

286 where  $S(t)$  describes the density of susceptible nodes,  $I(t)$  the density of infected nodes,  
 287  $Q(t)$  the density of quarantine nodes, and  $R(t)$  the density of recovered nodes at time  $t$ ,  
 288 respectively.



289

FIG. 5. Flow diagram of the *SIQRS* epidemic model.

290 In Figure 5 the flow diagram of the *SIQRS* epidemic model is described and the transitions  
 291 between the different states are explained bellow:

292 **S**  $\rightarrow$  **I** : A susceptible node is infected with probability  $\beta k \theta$ . In which  $\beta$  is the  
 293 infective probability of the disease,  $k$  is the degree of the node and  $\theta$  is the  
 294 fraction of links over which the infection can spread. In other words, the  
 295 fraction of links pointing to infected nodes. As such, a node is more likely  
 296 to contract the disease as its node degree is larger.

297 **S**  $\rightarrow$  **R**: Susceptible nodes become recovered (removed) with probability  $\alpha$ . In this  
 298 model we considered that several susceptible nodes have temporary immu-  
 299 nity, ether because of vaccination or natural immunity, in either case, the  
 300 immunity is only temporary.

301 **I**  $\rightarrow$  **Q**: To contain the spreading of the infection, infected nodes are quarantined  
 302 with probability  $\sigma$ .

303 **I** → **R**: Infected nodes recover spontaneously with probability  $\gamma$ .

304 **Q** → **R**: As a result of antiviral treatment or other mechanisms some of the quar-  
 305 antine nodes become recovered with probability  $\epsilon$  and this gives them a  
 306 temporary immunity.

307 **R** → **S**: With probability  $\delta$ , nodes in the recovered state lose their temporary im-  
 308 munity and become again susceptible nodes.

309 In analyzing the dynamics of the epidemic model we consider that the probability for  
 310 a node to become infected depends directly on its node degree. Additionally, since the  
 311 network connectivity is heterogeneous the presence of nodes with different degrees needs  
 312 to be taken into consideration. As such, it is convenient to assume that the population is  
 313 organized in classes. In particular, we will consider that within each class all nodes have the  
 314 same node degree  $k$ , with  $k \in [m : k_{max}]$  where  $k_{max}$  is the highest node degree value for  
 315 the entire network. Also, within each class, the nodes can be in only one of four different  
 316 compartments,  $S_k(t)$ ,  $I_k(t)$ ,  $Q_k(t)$  and  $R_k(t)$  which represent the densities of susceptible,  
 317 infected, quarantined and removed nodes with degree  $k$  at time  $t$ , respectively. Furthermore  
 318 the density of susceptible, infected, quarantined and recovered nodes in the entire network  
 319 is defined as:

$$S(t) = \sum_k S_k(t)P(k), \quad I(t) = \sum_k I_k(t)P(k),$$

$$Q(t) = \sum_k Q_k(t)P(k), \quad R(t) = \sum_k R_k(t)P(k).$$

320 Under the assumptions described above, the mean-field reaction rate dynamical equations  
 321 for class  $k$ , can be written as:

$$\begin{aligned} \frac{dS_k(t)}{dt} &= -\beta k S_k(t) \theta(t) - \alpha S_k(t) + \delta R_k(t) \\ \frac{dI_k(t)}{dt} &= \beta k S_k(t) \theta(t) - \gamma I_k(t) - \sigma I_k(t) \\ \frac{dQ_k(t)}{dt} &= \sigma I_k(t) - \epsilon Q_k(t) \\ \frac{dR_k(t)}{dt} &= \gamma I_k(t) + \epsilon Q_k(t) + \alpha S_k(t) - \delta R_k(t) \end{aligned} \tag{15}$$

323 where the fraction  $\theta(t)$  of links pointing to infected nodes is given by

$$\theta(t) = \frac{\sum_k k P(k) I_k(t)}{\sum_s P(s)} = \frac{1}{\bar{k}} \sum_k k P(k) I_k(t). \tag{16}$$

325 in which  $P(k)$  is the degree distribution and  $\bar{k}$  is the average degree within the network and  
 326 denotes the normalization factor.

327 In order to get the equilibrium solution in steady state,  $E_+(S_k^\infty, I_k^\infty, Q_k^\infty, R_k^\infty)$ , is needed  
 328 make the right side of equation (7) equals to zero,

$$\begin{aligned}
 & -\beta k S_k^\infty \theta^\infty - \alpha S_k^\infty + \delta R_k^\infty = 0 \\
 & \beta k S_k^\infty \theta^\infty - \gamma I_k^\infty - \sigma I_k^\infty = 0 \\
 & \sigma I_k^\infty - \epsilon Q_k^\infty = 0 \\
 & \gamma I_k^\infty + \epsilon Q_k^\infty + \alpha S_k^\infty - \delta R_k^\infty = 0
 \end{aligned} \tag{17}$$

330 with,

$$\theta^\infty = \frac{\sum_k k P(k) I_k^\infty}{\bar{k}}. \tag{18}$$

332 Solving for  $S_k^\infty$ ,  $Q_k^\infty$  and  $R_k^\infty$  we obtain,

$$\begin{aligned}
 S_k^\infty &= \frac{\gamma + \sigma}{\beta k \theta^\infty} I_k^\infty \\
 Q_k^\infty &= \frac{\sigma}{\epsilon} I_k^\infty \\
 R_k^\infty &= \frac{\beta k \theta^\infty + \alpha}{\delta} S_k^\infty \\
 &= \frac{(\beta k \theta^\infty + \alpha)(\gamma + \sigma)}{\delta \beta k \theta^\infty} I_k^\infty.
 \end{aligned} \tag{19}$$

338 Taking into account the normalization condition

$$S_k^\infty + I_k^\infty + Q_k^\infty + R_k^\infty = 1, \tag{20}$$

340 and substituting equation (19) in equation (20), we obtain for  $I_k^\infty$

$$I_k^\infty \left[ \frac{\gamma + \sigma}{\beta k \theta^\infty} + \frac{\sigma}{\epsilon} + \frac{(\beta k \theta^\infty + \alpha)(\gamma + \sigma)}{\delta \beta k \theta^\infty + 1} \right] = 1, \tag{21}$$

$$I_k^\infty = \frac{\delta \beta k \theta^\infty}{\beta k \theta^\infty [\delta(1 + \frac{\sigma}{\epsilon}) + (\gamma + \sigma)] + (\gamma + \sigma)(\delta + \alpha)}. \tag{22}$$

343 Then, inserting equation (22) in equation (18), one gets

$$\begin{aligned}
 \theta^\infty &= \frac{1}{\bar{k}} \sum_k \frac{\delta \beta k^2 P(k) \theta^\infty}{\beta k \theta^\infty [\delta(1 + \frac{\sigma}{\epsilon}) + (\gamma + \sigma)] + (\gamma + \sigma)(\delta + \alpha)} \\
 &\triangleq f(\theta^\infty).
 \end{aligned} \tag{23}$$



Obviously, the last equation has a trivial solution  $\theta^\infty = 0$ . To ensure that equation (23) has a non trivial solution, that is  $0 < \theta^\infty \leq 1$ . The following conditions must be both satisfied

$$\left[ \frac{df(\theta^\infty)}{d\theta^\infty} \right]_{\theta^\infty=0} > 1, \quad f(1) \leq 1,$$

so, we have

$$\frac{\delta\beta}{(\alpha + \delta)(\gamma + \sigma)} \frac{\bar{k}^2}{\bar{k}} > 1$$

We can obtain the epidemic threshold  $\beta_c$  using the last equation as,

$$\frac{\delta\beta}{(\alpha + \delta)(\gamma + \sigma)} \frac{\bar{k}^2}{\bar{k}} > 1,$$

$$\beta > \underbrace{\left(1 + \frac{\alpha}{\delta}\right)(\gamma + \sigma)}_{\beta_c} \frac{\bar{k}}{\bar{k}^2}.$$

346 as it can be seen, the epidemic threshold  $\beta_c$  depends on the fluctuations in the degree  
 347 distribution and mean degree of the network. And, if  $\beta < \beta_c$  the epidemic disappears, in  
 348 otherwise an epidemic outbreak occurs.

## 349 B. Quarantine jointly with *self-quarantine* process

350 In the epidemic model described before, is considered that only infected individuals can be  
 351 quarantined. However, in a real scenario individuals tend to protect themselves by avoiding  
 352 contacts with infected individuals temporally, we call this process *self-quarantine*. In this  
 353 sense, the flow diagram of the SIQRS model is shown in Fig. 6, where  $\eta$  describes the  
 354 probability that a susceptible individual is quarantined. Then, the mean-field reaction rate  
 355 dynamical equations for class  $k$  (Eq. 15), takes the form:

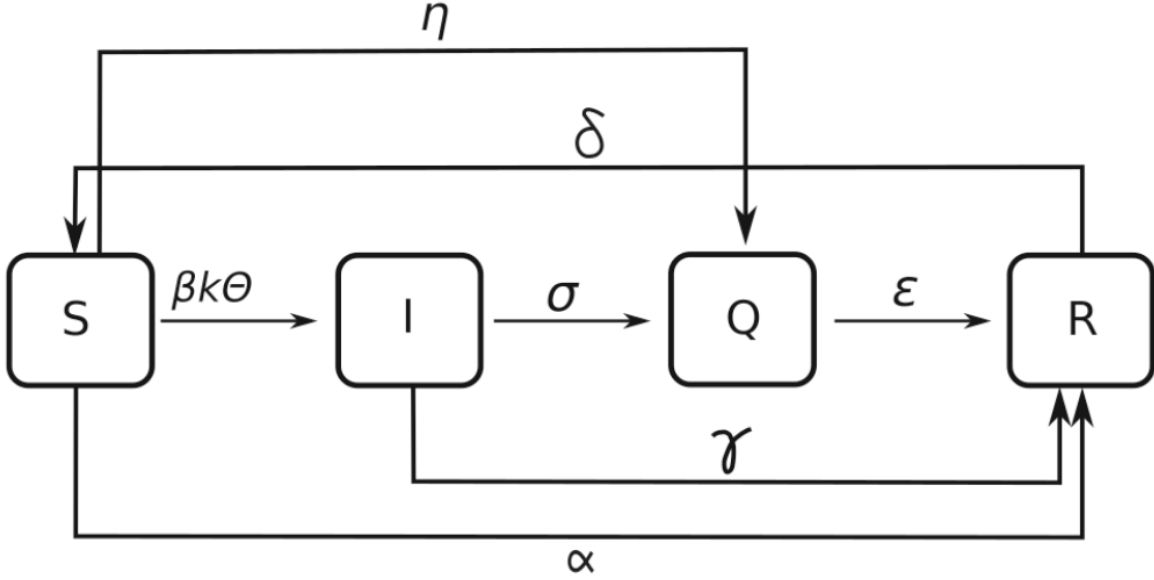
$$\begin{aligned} \frac{dS_k(t)}{dt} &= -\beta k S_k(t) \theta(t) - (\alpha + \eta) S_k(t) + \delta R_k(t) \\ \frac{dI_k(t)}{dt} &= \beta k S_k(t) \theta(t) - \gamma I_k(t) - \sigma I_k(t) \\ \frac{dQ_k(t)}{dt} &= \sigma I_k(t) - \epsilon Q_k(t) \\ \frac{dR_k(t)}{dt} &= \gamma I_k(t) + \epsilon Q_k(t) + (\alpha + \eta) S_k(t) - \delta R_k(t) \end{aligned}, \quad (24)$$

357 the density  $I_k^\infty$  and the epidemic threshold, take the form:

$$358 \quad I_k^\infty = \frac{\delta\beta k \theta^\infty}{\beta k \theta^\infty \left[ \delta \left(1 + \frac{\sigma}{\epsilon}\right) + (\gamma + \sigma) \right] + (\gamma + \sigma)(\delta + (\alpha + \eta))}. \quad (25)$$

$$\beta > \underbrace{\left(1 + \frac{(\alpha + \eta)}{\delta}\right)(\gamma + \sigma)}_{\beta_c} \frac{\bar{k}}{k^2},$$

359 respectively.



360

FIG. 6. Flow diagram of the *SIQRS* epidemic model including the *self-quarantine* process.

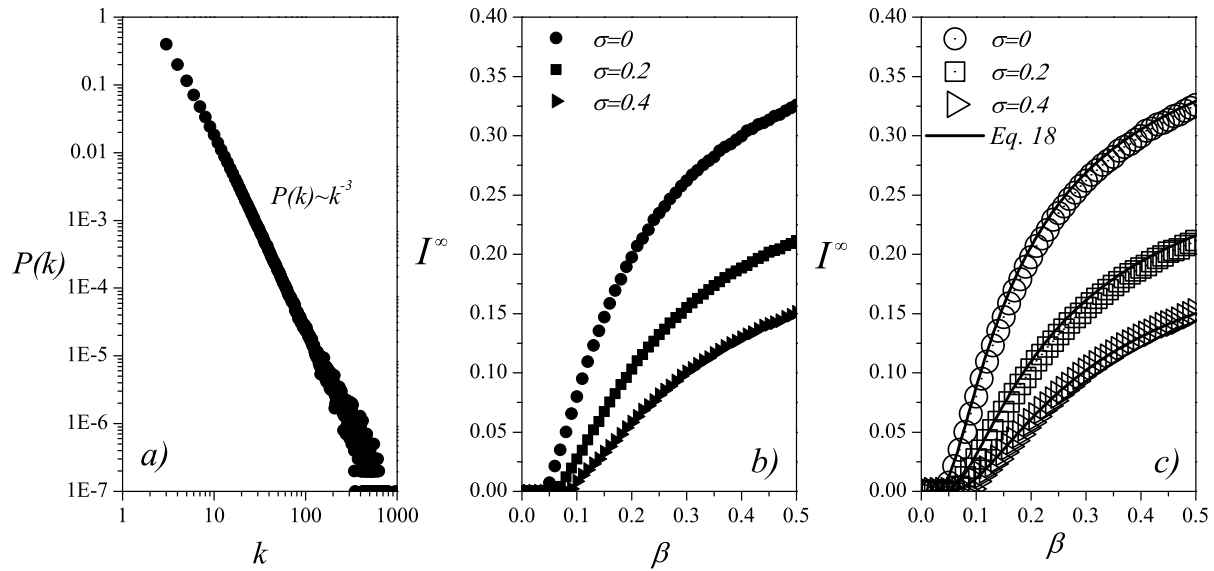
### 361 C. Quarantine in joint with *deleting-infected-links* process

362 Another process present in a real scenario is that several susceptible individuals can dis-  
363 connect permanently of its neighbor infected individuals. In order to investigate the impact  
364 of this process, we include the probability  $\psi$  that one susceptible individual disconnects from  
365 its neighbor infected individuals. In this case, the flow diagram is the same of Fig. 6, but  
366 due to the fluctuation of the degree in the network, the  $\theta$  probability also depends on  $\psi$ .

## 367 IV. NUMERICAL RESULTS

368 In order to investigate the effect of network topology on the steady state behavior of the  
369 proposed *SIQRS* epidemic models we chose the parameter set  $\alpha = 0.1$ ,  $\delta = 0.4$ ,  $\gamma = 0.5$ ,  
370 and  $\epsilon = 0.6$  and let the influence of the node degree and the probability of quarantine vary  
371 between  $\sigma = 0, 0.2, 0.4$  and  $\beta = 0.01, 0.02, \dots, 0.5$ , respectively. As a point of comparison,

372 we first investigate the case with the quarantine as the only control process and using a  
 373 scale-free network with degree distribution following a power-law exponent  $\nu = 3$ . That is,  
 374 the underlining network is a realization of the classical *BA* model. The simulations were for  
 375 networks of 10000 nodes with  $m = 3$  and three values for  $\sigma = 0, 0.2$  and  $0.4$ . The dynamics  
 376 of the spreading process were started with an initial infection of  $I_0 = 100$  nodes, the infected  
 377 nodes were selected randomly. It is important to mention that, each simulation was repeated  
 378 1000 times and averaged the results obtained are presented in Figure 7.



379

380 FIG. 7. a) Degree distribution of the network. b) Relation between  $I^\infty$  and  $\beta$  with  $\sigma = 0, 0.2$  and  
 381 0.4. c) Comparison between numerical simulations and the analytical solution given by equation  
 382 (31).  
 383

384

385 In particular, Figure 7a) shows the degree distribution of the network considered in the  
 386 simulations, as can be seen the degree distribution  $P(k) \sim k^{-3}$  as expected for a realization  
 387 of the *BA* model. Figure 7b) shows the relation between  $I^\infty$  and  $\beta$  for three different values  
 388 of  $\sigma = 0, 0.2$  and  $0.4$ . As it can be seen, as the quarantine rate  $\sigma$  increases, the density of  
 389 infected nodes decreases for all values of  $\beta$ .

390 In order to validate the results indicated by the numerical simulations, an analytical  
 391 solution is derived for  $I^\infty = \sum_k I_k^\infty(t)P(k)$  using equations (22), (23) and the values of  
 392 the degree distribution  $P(k)$  and the average degree  $\bar{k}$  of the network. For the networks

393 generated using the *BA* model<sup>16</sup> we have:

$$394 \quad P(k) \sim 2m^2k^{-3}, \quad \bar{k} = \int_m^\infty kP(k) = 2m. \quad (26)$$

395 Substituting equation (26) in equation (23) we get,

$$396 \quad \theta^\infty = m\theta^\infty$$

$$397 \quad \sum_k \frac{\delta\beta}{k [\beta k \theta^\infty [\delta(1 + \frac{\sigma}{\epsilon}) + (\gamma + \sigma)] + (\gamma + \sigma)(\delta + \alpha)]}. \quad (27)$$

399 Integrating over all  $k$  values, results in

$$400 \quad \frac{1}{m} = \beta\delta \lim_{b \rightarrow \infty}$$

$$401 \quad \int_m^b \frac{1}{k [\beta k \theta^\infty [\delta(1 + \frac{\sigma}{\epsilon}) + (\gamma + \sigma)] + (\gamma + \sigma)(\delta + \alpha)]} dk, \quad (28)$$

403 and solving for  $\theta^\infty$ , we obtain

$$404 \quad \theta^\infty = \frac{(\gamma + \sigma)(\delta + \alpha)}{m\beta [\delta(1 + \frac{\sigma}{\epsilon}) + (\gamma + \sigma)] \left[ e^{\frac{(\gamma + \sigma)(\delta + \alpha)}{m\beta\delta}} - 1 \right]}. \quad (29)$$

405 Using equation (29) and (22) and integrating for all  $k$  values, we obtain for  $I^\infty$  as,

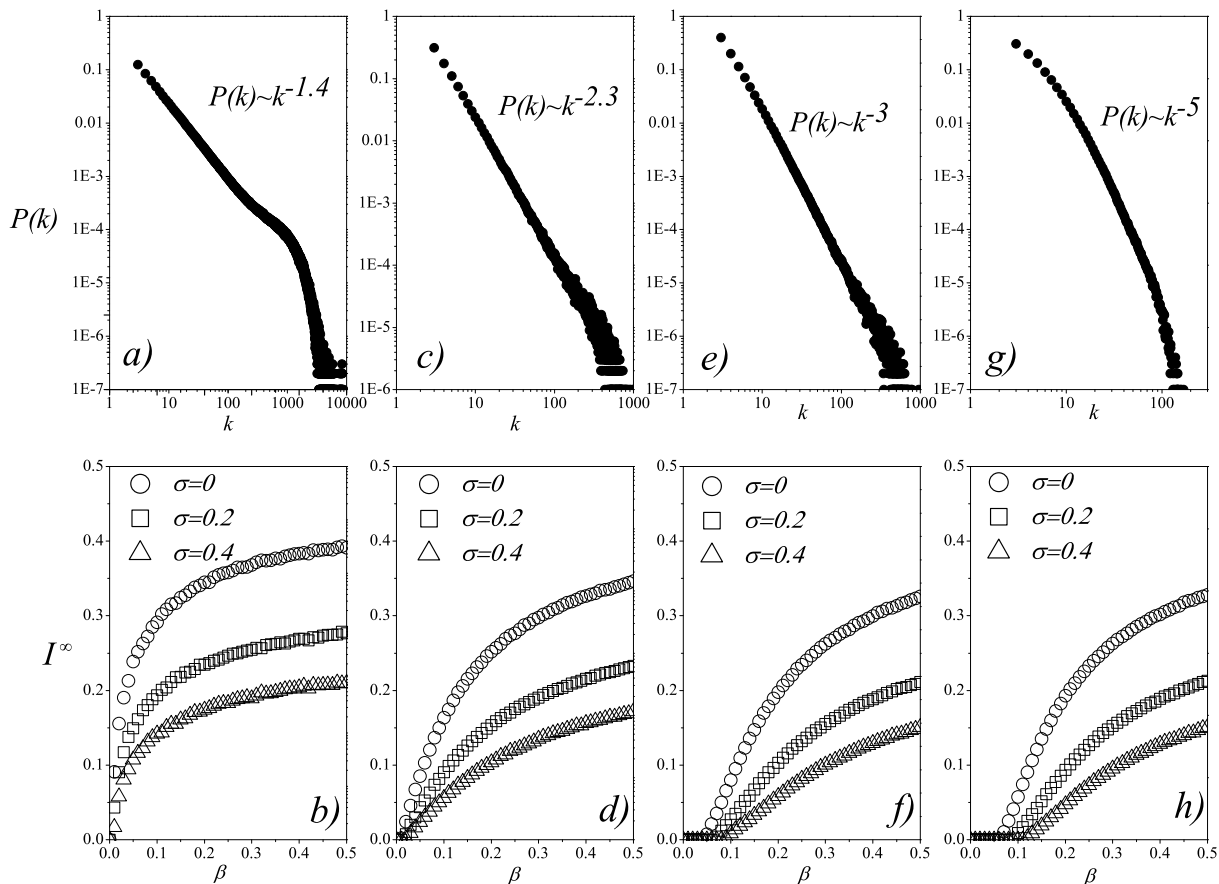
$$406 \quad I^\infty = \frac{2m^2\beta\delta}{\delta(1 + \frac{\sigma}{\epsilon}) + (\gamma + \sigma)}$$

$$407 \quad \lim_{b \rightarrow \infty} \int_m^b \frac{dk}{k^2 \left[ k + m \left( e^{\frac{(\gamma + \sigma)(\delta + \alpha)}{m\beta\delta}} - 1 \right) \right]} dk, \quad (30)$$

$$409 \quad I^\infty = \frac{2 \left[ m\beta\delta \left( e^{\frac{(\gamma + \sigma)(\delta + \alpha)}{m\beta\delta}} - 1 \right) - (\gamma + \sigma)(\delta + \alpha) \right]}{m\beta \left( e^{\frac{(\gamma + \sigma)(\delta + \alpha)}{m\beta\delta}} - 1 \right)^2 [\delta(1 + \frac{\sigma}{\epsilon}) + (\gamma + \sigma)]} \quad (31)$$

410 Figure 7c) shows that the analytical predictions 31 and the numerical simulations fit appro-  
411 priately.

412 With the aim of analyze the effect of the network topology on the quarantine efficiency,  
 413 we repeat the previous simulations but using scale-free networks with power-law exponents  
 414  $\nu = 1.4, 2.3$  and  $5$ . For the growth of these networks, we use the Model I with  $p = 0.3$  and  
 415  $p = 0.7$  and the Model II with  $A = 6$  respectively.



416

417 FIG. 8. Comparison of the densities  $I^\infty$  retrieved from the simulations for different values of  $\beta$ ,  $\sigma$   
 418 and  $\nu$ .

419 In Figure 8 are shown the results of the simulations described above. In 8a and 8b are  
 420 showed the degree distribution of the network with  $\nu \sim 1.4$  and the relation between  $I^\infty$   
 421 and  $\beta$  obtained from the *SIQRS* model over this network. Similarly, in Figs. 8c and 8d for  
 422 the network with  $\nu \sim 2.3$ , Figs. 8e and 8f for the network with  $\nu \sim 3$  and Figs. 8g and 8h  
 423 for the network with  $\nu \sim 5$ .

424 As it can be seen in Figs. 8b, 8d, 8f and 8h, as the exponent  $\nu$  decreases, the density  
 425  $I^\infty$  increases significantly for all the  $\sigma$  values. In contrary, for  $\nu = 3$  and  $\nu = 5$ , the density  
 426  $I^\infty$  have a similar behavior as  $\beta$  increases. Another interesting phenomenon is that, for

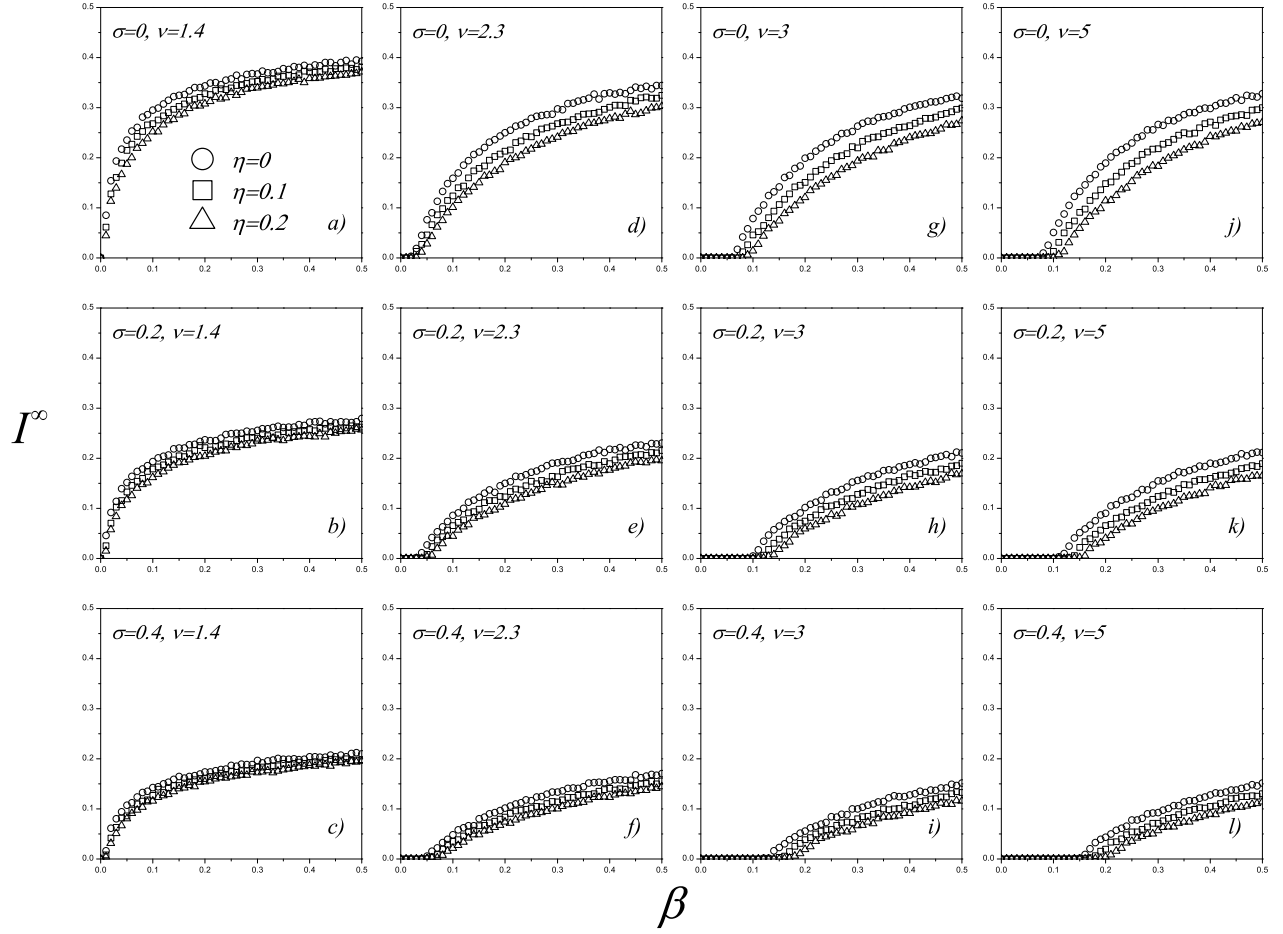


FIG. 9. Comparison of the densities  $I^\infty$  retrieved from the simulations for different values of  $\beta$ ,  $\sigma$ ,  $\nu$  and  $\eta$ .

427  $\nu = 5$ ,  $I^\infty$  starts to grow later than for  $\nu = 3$ . A possible cause for this behavior is that,  
 428 as the exponent  $\nu$  increases, the quantity of nodes hardly connected decreases and as a  
 429 consequence, the emergence of super spreader nodes is less likely for  $\beta \approx 0$ .

430 In order to investigate the efficiency of quarantine in joint with the *self-quarantine* process  
 431 we reproduce the numerical simulations of the Fig. 8 including the *self-quarantine* process  
 432 with  $\eta = 0, 0.1, 0.2$ . The results of the numerical simulations are showed in Figure 9. In  
 433 Figure 9a, 9b and 9c is showed the  $I^\infty$  obtained using the complex network with power-law  
 434 exponent  $\nu \sim 1.4$  defining  $\sigma = 0, 0.2$  and  $0.4$  respectively, and with  $\eta = 0, 0.1, 0.2$ . Similarly  
 435 for  $\nu \sim 2.3$  in Figs. 9d, 9e, 9f, for  $\nu \sim 3$  in Figs. 9g, 9h, 9i and for  $\nu \sim 5$  in Figs. 9j,  
 436 9k, 9l. As can be seen, in all the cases the density of infected individuals decreases as the

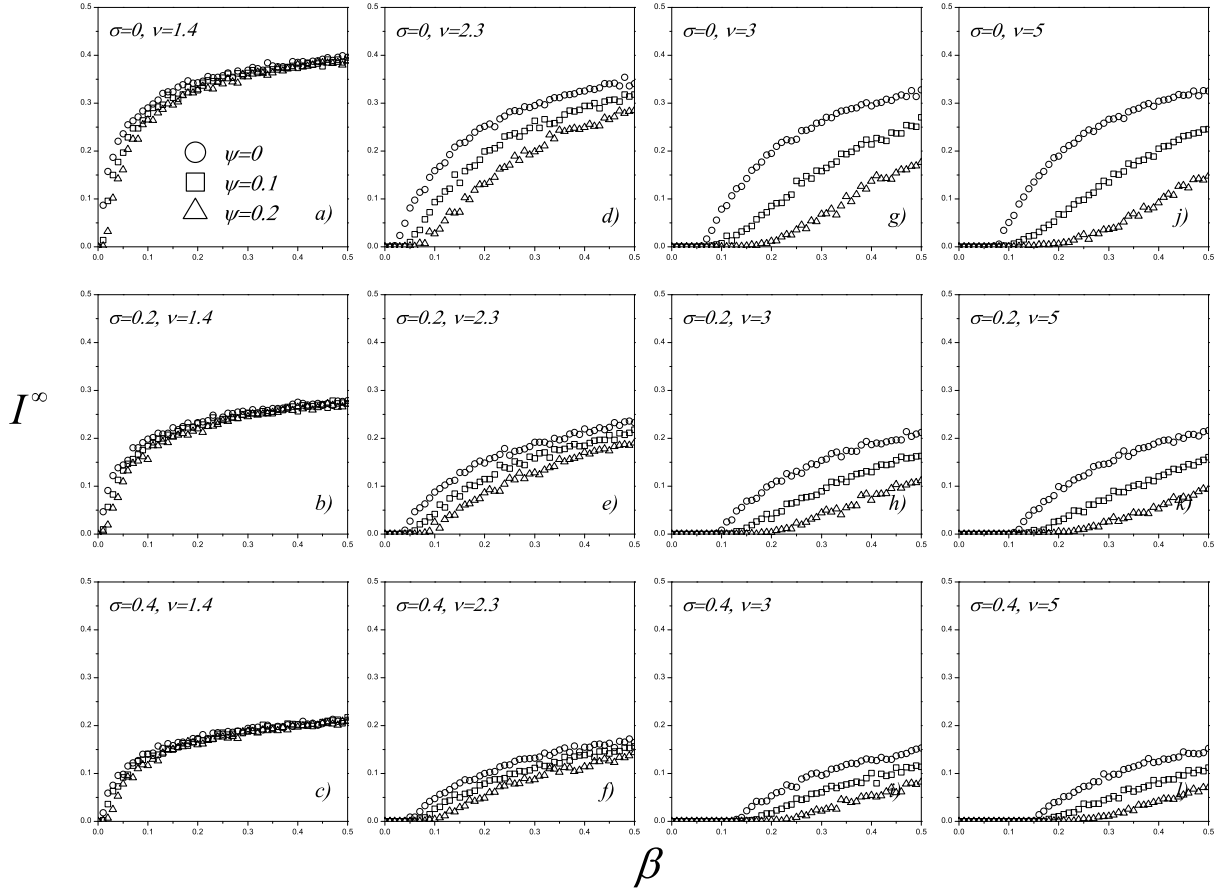


FIG. 10. Comparison of the densities  $I^\infty$  retrieved from the simulations for different values of  $\beta$ ,  $\sigma$ ,  $\nu$  and  $\psi$ .

439  $\eta$  probability increases. However, the best efficiency in the contain the spread is obtained  
 440 when the *self-quarantine* process and the quarantine as a global process are implemented in  
 441 joint. Finally, to investigate the efficiency of quarantine in joint with the *deleting-infected-*  
 442 *links* process we reproduce the numerical simulations of the Fig. 8 including the probability  
 443  $\psi = 0, 0.1, 0.2$  in the spreading process. The results of the numerical simulations are showed  
 444 in Figure 10. In Figure 10a, 10b and 10c is showed the  $I^\infty$  obtained using the complex  
 445 network with power-law exponent  $\nu \sim 1.4$  defining  $\sigma = 0, 0.2$  and  $0.4$  respectively, and with  
 446  $\psi = 0, 0.1, 0.2$ . Similarly for  $\nu \sim 2.3$  in Figs. 10d, 10e, 10f, for  $\nu \sim 3$  in Figs. 10g, 10h,  
 447 10i and for  $\nu \sim 5$  in Figs. 10j, 10k, 10l. As can be seen, in all the cases the density of  
 448 infected individuals decreases as the  $\psi$  probability increases. However, the best efficiency in  
 449 the contain the spread is obtained when the *deleting-infected-links* and the quarantine as a

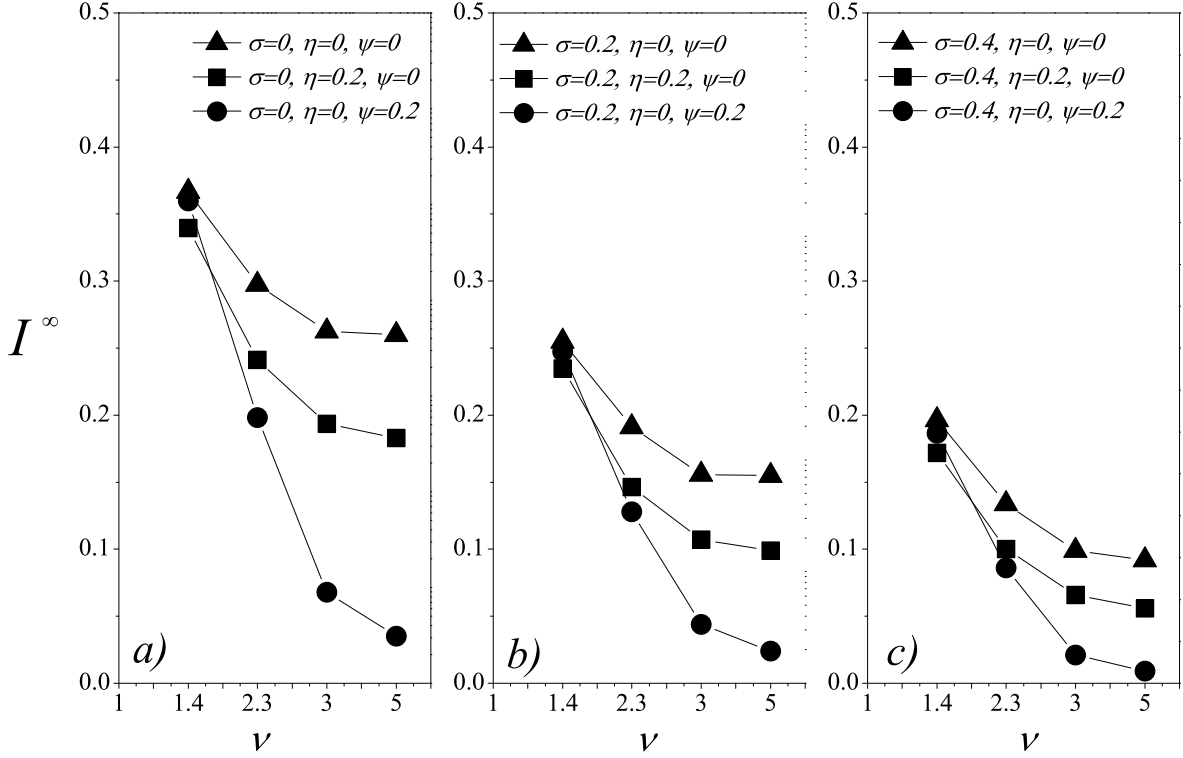


FIG. 11. Relation between the density  $I^\infty$  and the power-law exponent  $\nu$  for  $\beta = 0.3$ , and different values for  $\sigma$ ,  $\eta$  and  $\psi$ .

450 global processes are implemented together. The previous results indicate that quarantine is  
 452 an effective measure to contain the spread of a disease, however its effectiveness increases if it  
 453 is combined with the implementation of some *self-protection* process by the individuals of the  
 454 population. Figure 11 shows a clearer view of this conclusion. That is, in Fig. 11 is showed  
 455 the relation between the density  $I^\infty$  and the power-law exponent  $\nu$  of the degree distribution  
 456 in the network. From the figure, it is possible to see that the worst efficiency (solid triangles)  
 457 is obtained when the quarantine is defined as the only control action. However, when it is  
 458 combined with *self-protection* processes as the *self-quarantine* (solid squares) and *deleting-*  
 459 *infected-links* (solid circles) processes the best efficiency is obtained.



## 460 V. CONCLUDING REMARKS

461 In summary, in this paper we have investigated the efficiency of the quarantine policy  
462 in networks with different topologies. More precisely, we have proposed a *SIQRS* epidemic  
463 model and we measured the density of infected individuals in steady state generated with  
464 that model in networks with degree distribution following a power-law  $P(k) \sim k^{-\nu}$  with  
465 different  $\nu$  values. We found that the efficiency of the *SIQRS* model is strongly related  
466 with the  $\nu$  value. More exactly, we found that as the exponent  $\nu$  decreases lower three, the  
467 efficiency of the quarantine decreases. Also, in this paper we investigated the efficiency of  
468 the quarantine in joint with *self-protection* processes and we found that the addition of self-  
469 protection process improves the efficiency in containing the spread of the disease. That is,  
470 the density of infected individuals in steady state considerably reduces. This result implies  
471 that the awareness of the population through social health programs can be a good strategy  
472 to reduce the number of infected individuals during the spread of a disease.

473 **Acknowledgments:** This work was supported in part by CONACYT, National Research  
474 Council of México under postdoctoral grand number: 291053.

475 **Competing interest:** The authors declares that there is no conflict of interest regarding  
476 the publication of this paper.

## 477 REFERENCES

478 <sup>1</sup>Tan S., Lü J., and Lin Z., Emerging Behavioral Consensus of Evolutionary Dynamics on  
479 Complex Networks, *SIAM J. Control Optim.*, 54(6): 3258–3272, 2016.

480 <sup>2</sup>Lü J. and Chen G., A time-varying complex dynamical network model and its controlled  
481 synchronization criteria, *IEEE Trans. Automat. Contr.*, 50(6): 841–846, 2005.

482 <sup>3</sup>Chen Y., Lü J., Yu X. and Lin Z., Consensus of discrete-time second-order multiagent  
483 systems based on infinite products of general stochastic matrices, *SIAM J. Control Optim.*,  
484 51(4): 3274–3301, 2013.

485 <sup>4</sup>Anderson R.M. and May R.M., *Infectious Diseases of Humans: Dynamics and Control*,  
486 Oxford University Press 1992.

487 <sup>5</sup>Granell C., Gomez S. and Arenas A., Dynamical Interplay between Awareness and Epi-  
488 demic Spreading in Multiplex Networks, *Phys. Rev. Lett.* 111(12), 128701, 2013.

- 489 <sup>6</sup>Granell C., Gomez S. and Arenas A., Competing spreading processes on multiplex net-  
490 works: Awareness and epidemics, *Phys. Rev. E*, 90, 012808, 2014.
- 491 <sup>7</sup>Jia-Qian K. and Hai-Feng Z., Effects of awareness diffusion and self-initiated awareness  
492 behavior on epidemic spreading - An approach based on multiplex networks, *Commun.*  
493 *Nonlinear Sci. Numer. Simulat.*, 44, 193–203, 2017.
- 494 <sup>8</sup>Fu X., Small M., and Chen G., *Propagation Dynamics on Complex Networks: Models,*  
495 *Methods and Stability Analysis*, Willey, United Kingdom, 2014.
- 496 <sup>9</sup>Kiss I.Z., Miller J.C. and Simon P.L., *Mathematics of Epidemic Networks*, Springer Inter-  
497 national Publishing, 2017.
- 498 <sup>10</sup>Lü J., Yu X. and Chen G., *Complex Systems and Networks: Dynamics, Controls and Ap-*  
499 *plications*, Springer-Verlag Berlin Heidelberg, 2016.
- 500 <sup>11</sup>Bailey N.T., *The Mathematical Theory of Infectious Diseases*, Charles Griffin & Company  
501 Ltd, 1975.
- 502 <sup>12</sup>Diekmann O. and Heesterbeek J.A.P., *Mathematical Epidemiology of Infectious Diseases*,  
503 Wiley 2000.
- 504 <sup>13</sup>Beretta E. and Takeuchi Y., Global stability of an SIR epidemic model with time delays.  
505 *J. Math. Biol.* **33**: 250. doi:10.1007/BF00169563, (1995).
- 506 <sup>14</sup>Liljeros F., Edling C., Amaral R., Nunes L. A., Stanley H. E., and Aberg Y., The web of  
507 human sexual contacts. *Nature*, 411, 907–908 doi:10.1038/35082140, 2001.
- 508 <sup>15</sup>Li T., Wang Y. and Guan Z.H., Spreading dynamics of a *SIQRS* epidemic model on  
509 scale-free networks. *Commun. Nonlinear Sci. Numer. Simulat.*, 19(3), 686–692, 2014.
- 510 <sup>16</sup>Barabási A.L., Albert R. and Jeong H., Mean-field theory for scale-free random networks.  
511 *Physica A* 272173-187, 1999.
- 512 <sup>17</sup>Liu J. and Zhang T., Epidemic spreading of an SEIRS model in scale-free networks. *Com-*  
513 *mun. Nonlinear Sci. Numer. Simulat.*, 16, 3375–3384, 2011.
- 514 <sup>18</sup>Albert R. and Barabási A.L., Statistical mechanics of complex networks. *Rev. Mod. Phys.*,  
515 74-1, 47–94, 2002.
- 516 <sup>19</sup>Shang J., Liu L., Li X., Xie F. and Wu C., Epidemic spreading on complex networks with  
517 overlapping and non-overlapping community structure, *Physica A*. 419: 171–182, 2015.
- 518 <sup>20</sup>Dorogovtsev S.N., Mendes J.F.F. and Samukhin A.N., Structure of growing networks:  
519 Exact solution of the Barabasi-Albert model. *Phys. Rev. Lett.* 85, 4633–4636, 2000.
- 520 <sup>21</sup>Barabási A.L., Albert R., and Jeong H., Mean-field theory for scale-free random networks,

521 *Physica A*, 272(1): 173–187, 1999.